



ELSEVIER

Journal of Alloys and Compounds 300–301 (2000) 267–274

Journal of  
ALLOYS  
AND COMPOUNDS

www.elsevier.com/locate/jallcom

# Laser-induced luminescence of rare-earth elements in natural zircon

M. Gaft<sup>a,\*</sup>, G. Panczer<sup>b</sup>, R. Reisfeld<sup>c</sup>, I. Shinno<sup>d</sup><sup>a</sup>Department of Natural Science, The Open University of Israel, 16 Klausner St., Tel-Aviv, Israel<sup>b</sup>Physical Chemistry of Luminescence Materials Laboratory, Lyon 1 University and CNRS, 43 Bd. Du 11 November 1918, 69622 Villeurbanne, France<sup>c</sup>Department of Inorganic and Analytical Chemistry, Hebrew University, 91940, Jerusalem, Israel<sup>d</sup>Laboratory of Earth Science, Kyushu University, Ropponmatsu, Fukuoka, Japan

## Abstract

Natural and synthetic zircons are investigated by time-resolved and high-resolution laser-induced luminescence to detect and ascribe various luminescence lines to a variety of rare-earth elements (REE). The selectivity of detection is possible by using different time delays after excitation, different gate widths and different excitation wavenumbers. This allowed us to detect REE in samples where they are hidden by intrinsic luminescence and are not visible in the steady-state luminescence spectra. Luminescence of  $\text{Eu}^{3+}$ ,  $\text{Tb}^{3+}$ ,  $\text{Er}^{3+}$ ,  $\text{Ho}^{3+}$ ,  $\text{Pr}^{3+}$ ,  $\text{Tm}^{3+}$  and  $\text{Ce}^{3+}$  is detected even at low concentration of REE and in the presence of  $\text{Dy}^{3+}$ ,  $\text{Sm}^{3+}$  and  $\text{Gd}^{3+}$ . © 2000 Published by Elsevier Science S.A. All rights reserved.

**Keywords:** Zircon; REE; Luminescence

## 1. Introduction

Zircon, is a zirconium silicate,  $\text{ZrSiO}_4$ , with a tetragonal structure ( $I4_1/amd$ ) where in the unit cell there are four  $\text{SiO}_4^{4-}$  and four  $\text{ZrO}_8^{12-}$  groups. In nature, zircon is an accessory mineral almost always found in igneous, sedimentary and metamorphic rock. Zircon's crystal chemistry strongly favors the incorporation of REE in  $\text{Zr}^{4+}$  site. The REE impurities become luminescent in a crystallographic environment of the lattice. This property, coupled with the ability to form waveguides in this material by the technique of ion implantation [1], makes zircon of interest as a potential host material for laser waveguide cavities. Thus spectroscopic analysis of zircon is needed to identify possible laser transitions.

X-ray fluorescence spectrometry and inductively coupled plasma analysis reveal the presence in the zircons of all existing REE. The steady-state luminescence in natural zircons is dominated by broad emission arising from radiation-induced centers and narrow emission lines of  $\text{Dy}^{3+}$  only. These emissions obscure the spectra of other

REE [2,3]. The thermal treatment enables to solve this problem in certain cases using the fact that the intensity of broad band luminescence quickly decreases after heating at 700–800°C, while the intensities of the REE lines remain nearly constant [3–5]. Even after heating the samples not all the REE can be identified by steady-state spectroscopy since the weaker luminescence lines of certain REE are obscured by stronger luminescence of others. For example, luminescence of  $\text{Pr}^{3+}$  is difficult to detect because the lines of  $\text{Sm}^{3+}$ ,  $\text{Dy}^{3+}$  and  $\text{Nd}^{3+}$  hide its radiative transitions. In turn,  $\text{Tb}^{3+}$  conceals luminescence of  $\text{Tm}^{3+}$  and so on.

The purpose of this work is to examine the zircon by laser-induced time-resolved luminescence, which allows differentiation between luminescence centers with emission spectra in the same spectral range but with different decay times. The method involves recording the intensity in a specific time gate at a given delay after the excitation pulse, where both the delay and the gate width have to be carefully chosen. We selected the zircon with strong yellow broad band luminescence under steady-state excitation (photons or electrons), where luminescence of REE is not detected. Time-resolved spectroscopy allows to detect the previously unseen emission lines, which were hidden under broad band luminescence and to differentiate between separate rare-earth elements. For the correct interpretation of all the lines of REE, synthetic zircon standards doped with individual REE were also studied.

\*Corresponding author. Tel.: +972-3-646-0549; fax: +972-3-646-0682.

E-mail address: michael@shaked.openu.ac.il (M. Gaft)

Table 1

REE concentrations (ppm) in zircon (Kola Peninsula, Russia) determined by inductively coupled plasma analysis

Ce	Pr	Sm	Eu	Tb	Gd	Dy	Ho	Er	Tm
68	20	48	25	40	146	352	96	300	56

## 2. Experimental

The luminescence spectra were investigated under fourth harmonic of YAG (266 nm) and nitrogen (337 nm) laser excitations, which deliver pulses of 10 ns duration and 0.1 cm<sup>-1</sup> spectral width. The pulse energy has been maintained to about 40 and 10 mJ for YAG and nitrogen lasers, respectively. The spectra observed at the geometry of 90° was analyzed by INSTASPEC equipment, which enables acquisition of time-resolving spectra at the following conditions: delay times and strobe pulse duration 20 ns to 9 ms, spectral detection range 250–900 nm (1200 channels, spectral resolution 0.1–1 nm, gratings with 400 and 1200 lines mm<sup>-1</sup>), detector type-intensified CCD matrix.

The steady-state luminescence spectra were investigated with a Dilor XY multichannel micro-Raman spectrometer. The 458 and 488 nm lines of a Spectra Physics 2016 Argon laser were used for excitations. The spectra observed at the geometry of 90° were analyzed by EG&G intensified CCD multichannel detector and triple monochromator, which is used for Raman spectroscopy and has a much higher resolution than the normal spectrofluorimeters.

This paper is based on luminescence of zircon from Kola Peninsula, Russia, which exhibits all REE luminescence lines detected in zircons. REE concentrations in this sample determined by inductively coupled plasma analysis are presented in Table 1. The sample was checked by micro-Raman spectroscopy to ensure that it does not contain impurities of foreign minerals, which may serve as host matrix for REE luminescent centers.

For the correct interpretation of all the lines of REE, synthetic zircon standards doped with individual REE<sup>3+</sup> elements were prepared. Zircon crystals were grown in MoO<sub>3</sub>–Li<sub>2</sub>MoO<sub>4</sub> flux with 99.99% pure ZrO<sub>2</sub> and REE in the form of R<sub>2</sub>O<sub>3</sub> [3].

## 3. Results

### 3.1. Synthetic samples

Fig. 1 represents laser-induced luminescence spectra recorded from pure artificial zircons activated with REE which have luminescent lines connected with electron transitions from the same excited level (<sup>4</sup>F<sub>9/2</sub> for Dy<sup>3+</sup>,

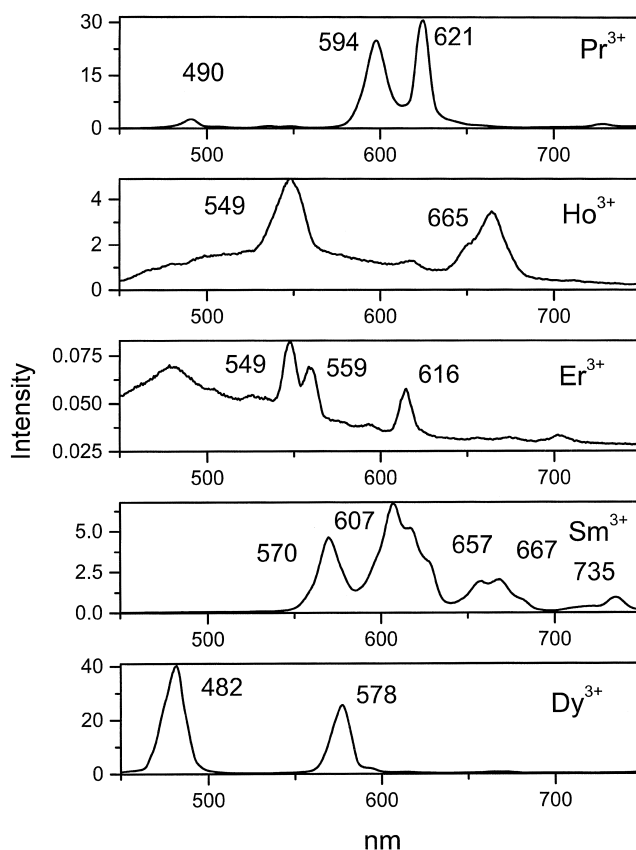


Fig. 1. Laser-induced luminescence spectra of ZrSiO<sub>4</sub> activated by Dy<sup>3+</sup>, Sm<sup>3+</sup>, Er<sup>3+</sup>, Ho<sup>3+</sup> and Pr<sup>3+</sup>.

<sup>4</sup>G<sub>5/2</sub> for Sm<sup>3+</sup>, <sup>4</sup>S<sub>3/2</sub> for Er<sup>3+</sup> and <sup>1</sup>D<sub>2</sub> for Pr<sup>3+</sup>) or from different levels (<sup>5</sup>S<sub>2</sub> and <sup>5</sup>F<sub>5</sub> for Ho<sup>3+</sup>), which have identical decay times. Consequently, the spectra are not changed with delay time, gate width and excitation energy and all luminescence lines of Sm<sup>3+</sup> are characterized by decay time of ~550 μs, Dy<sup>3+</sup>: 120 μs, Er<sup>3+</sup>: 25 μs, Pr<sup>3+</sup>: 10 μs, and Ho<sup>3+</sup>: 1 μs.

Fig. 2 represents luminescence spectra recorded from pure artificial zircon activated by Eu<sup>3+</sup>, Tb<sup>3+</sup> and Tm<sup>3+</sup>. These luminescent spectra in time-resolved experiment change with delay time and gate width. All luminescence lines of Eu<sup>3+</sup> are connected with electron transitions from the same <sup>5</sup>D<sub>0</sub> level, but their relative intensities are strongly dependent on the local site symmetry [6]. In time-resolved spectra of ZrSiO<sub>4</sub>:Eu two centers are detected with different excitations and decay times, one of which has very long decay of 1–2 ms, while the other has relatively short one of ~50 μs. The emission of Tb<sup>3+</sup> in the green part of the spectrum is connected with <sup>5</sup>D<sub>4</sub>–<sup>7</sup>F<sub>J</sub> transitions, with very long decay of ~2 ms, while the lines in the UV-violet part of the spectrum, with much shorter decay of ~350 μs, are connected with higher-level emission <sup>5</sup>D<sub>3</sub>–<sup>7</sup>F<sub>J</sub>. The emission of Tm<sup>3+</sup> is connected with <sup>1</sup>G<sub>4</sub>–<sup>3</sup>H<sub>6</sub> transition (482 nm) with decay time of ~120 μs, <sup>1</sup>D<sub>2</sub>–<sup>3</sup>H<sub>4</sub> transition (458 nm) with decay of ~5 μs, <sup>1</sup>I<sub>6</sub>–<sup>3</sup>H<sub>4</sub>

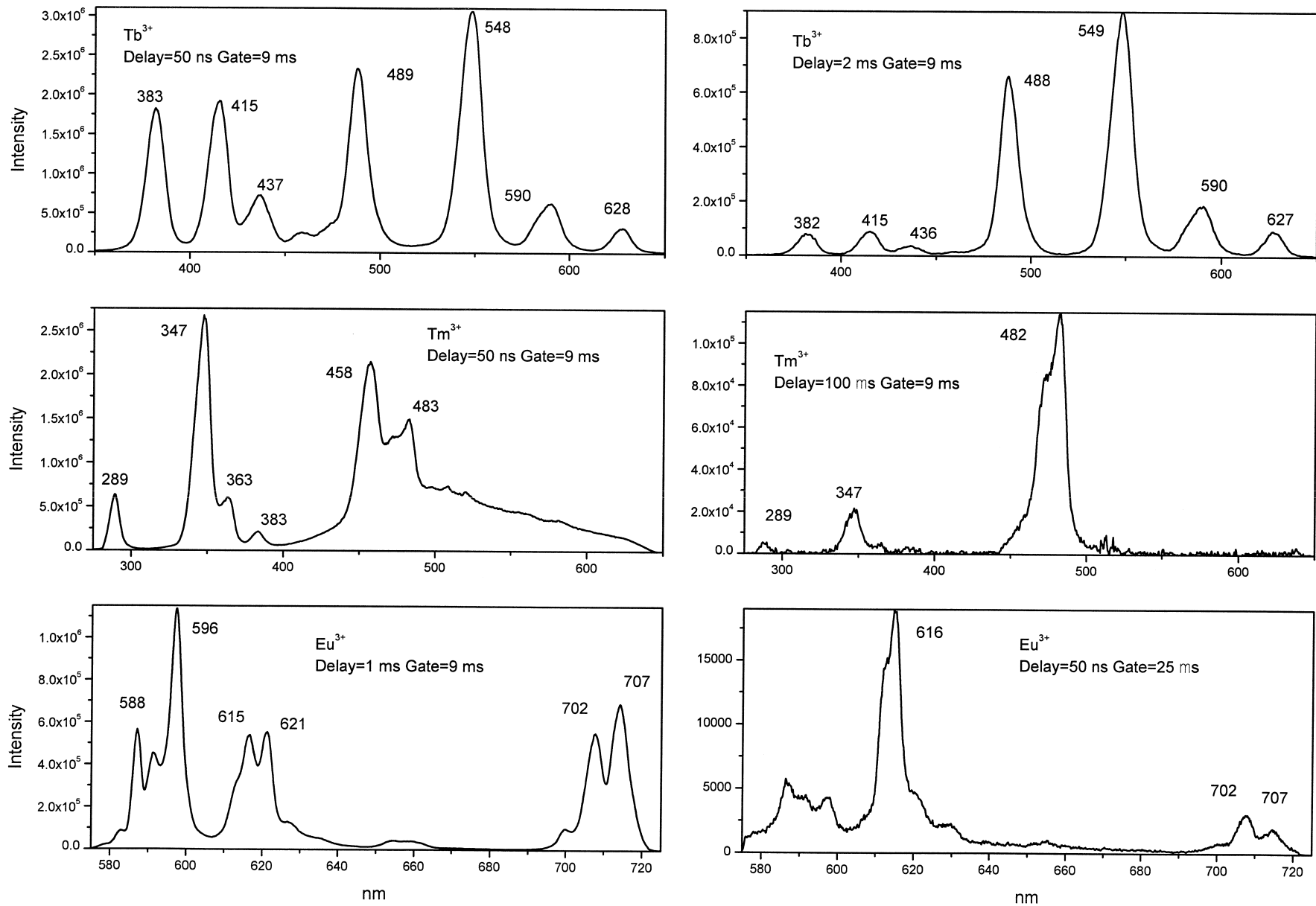


Fig. 2. Laser-induced luminescence spectra of ZrSiO<sub>4</sub> activated by Eu<sup>3+</sup>, Tb<sup>3+</sup> and Tm<sup>3+</sup>.

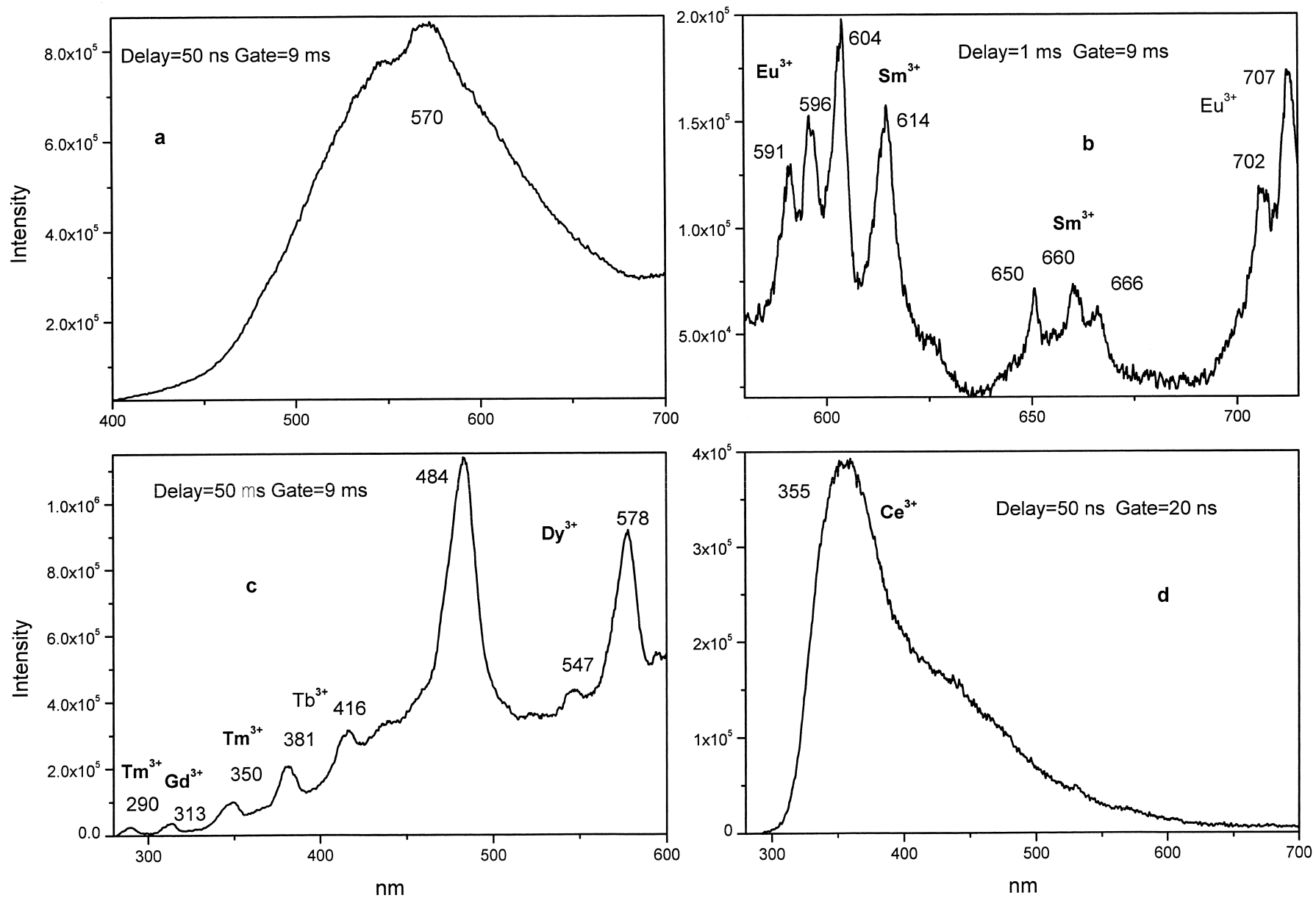


Fig. 3. Laser-induced time-resolved luminescence spectra of natural zircon (Kola Peninsula, Russia) under 337 nm (a, b) and 266 nm (c, d) excitations.

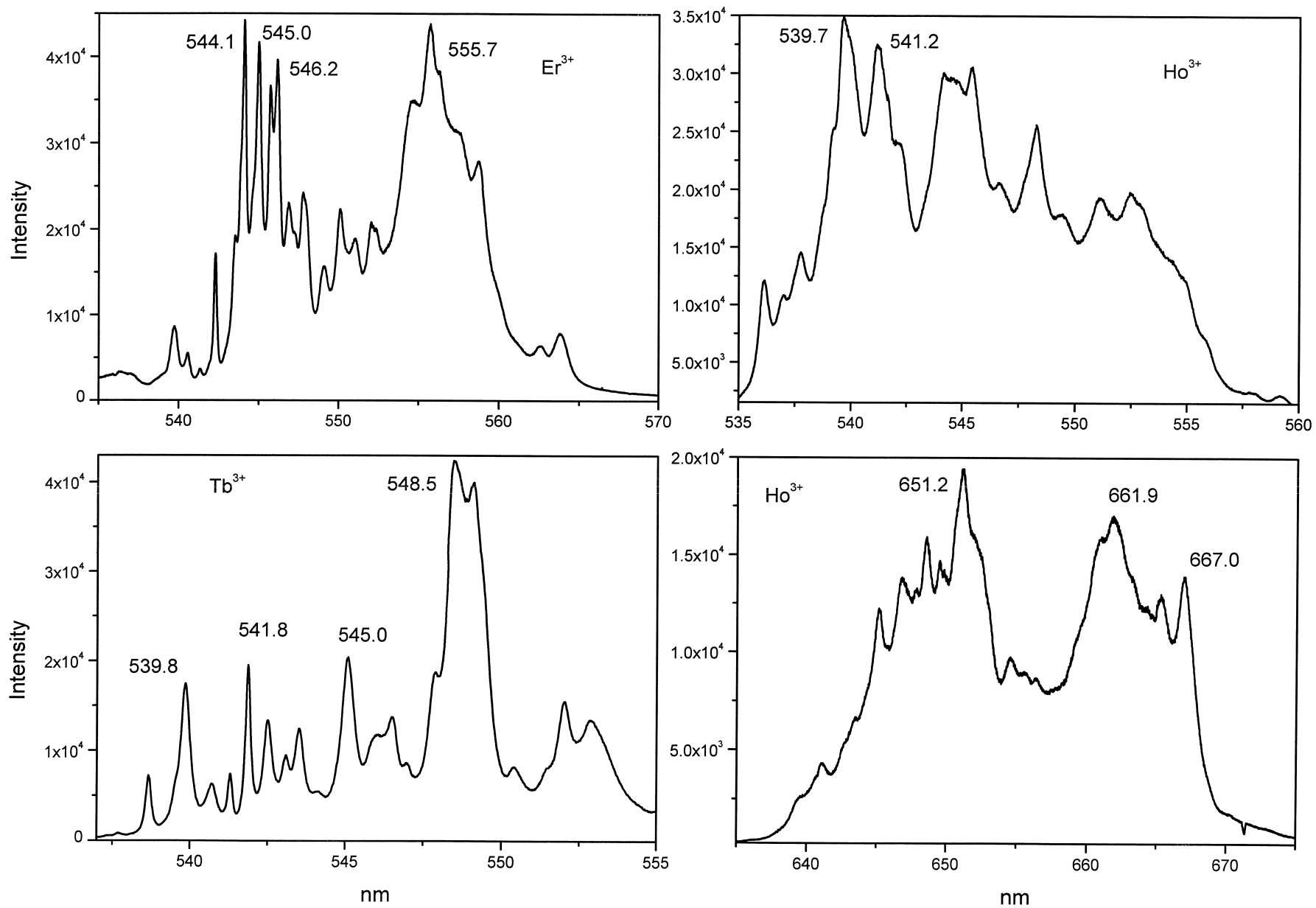


Fig. 4. Luminescence spectra of zircon activated by Er, Tb and Ho under 488 nm excitation.

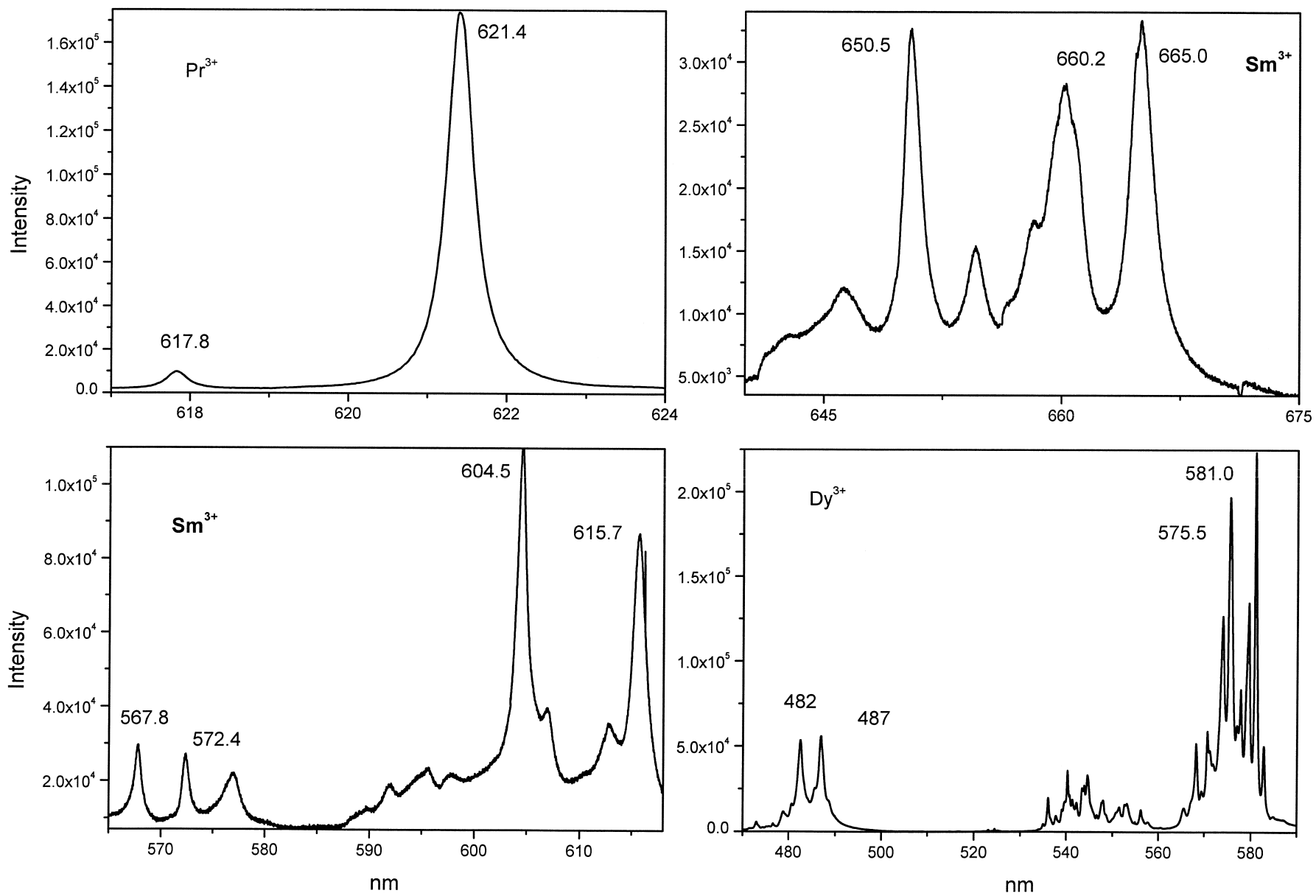


Fig. 5. Luminescence spectra of artificial zircon activated by Pr, Sm and Dy under 488 nm excitation.

and  ${}^1I_6 \rightarrow {}^3H_6$  transitions (347 and 289 nm) with decay of  $\sim 15 \mu\text{s}$ . Different decay times from these levels are evidently connected with nonradiative relaxation due to the presence of high frequency vibrations in the lattice [7].

### 3.2. Natural samples

We selected the natural zircon (Kola Peninsula, Russia) with broad-band yellow luminescence where REE luminescence is not detected under steady-state conditions (Fig. 3a). Relatively short delay time of  $100 \mu\text{s}$  allows to weaken broad bands with shorter decay of  $10\text{--}30 \mu\text{s}$  [4] and to detect the well-known lines of  $\text{Dy}^{3+}$  at 480 and 575 nm. Long delay of  $1\text{--}2 \text{ ms}$  enables to extinguish the yellow bands and to detect long-lived  $\text{Sm}^{3+}$  and  $\text{Eu}^{3+}$ –I luminescence (Fig. 3b). Time-resolved spectroscopy in the UV part of the spectrum enables to detect  $\text{Gd}^{3+}$  ( ${}^6P_{7/2} \rightarrow {}^8S_{7/2}$ ),  $\text{Tm}^{3+}$  and  $\text{Tb}^{3+}$  (Fig. 3c). Narrow band at 355 nm with a very short decay time of  $20\text{--}30 \text{ ns}$  is detected (Fig. 3d) which is most probably connected with  $\text{Ce}^{3+}$  luminescence.

Other REE, namely  $\text{Er}^{3+}$ ,  $\text{Ho}^{3+}$ , and  $\text{Pr}^{3+}$  are not detected under UV excitation even by time-resolved spectroscopy. The reason is that they have relatively short decay times similar to those of radiation-induced centers. Visible excitation, which is not effective for broad band luminescence, allows to reveal  $\text{Er}^{3+}$ ,  $\text{Ho}^{3+}$  and  $\text{Pr}^{3+}$  luminescence lines, using high-resolution steady-state spectroscopy. Figs. 4 and 5 represent steady-state luminescence spectra of artificial zircon activated by Er, Tb, Ho, Dy, Sm and Pr under 488 nm excitation. It is clearly seen that under such experimental conditions each element has

Table 2  
Characteristic lines of rare-earths in laser-induced luminescence of natural zircon

Center	$\lambda_{\text{lum}}$ (nm)	$\lambda_{\text{ex}}$ (nm)	$\tau$ ( $\mu\text{s}$ )	Transition
$\text{Ce}^{3+}$	355	266	$2 \times 10^{-2}$	${}^2D_{-2} \rightarrow {}^2F$
$\text{Pr}^{3+}$	489	337	1	${}^1P_0 \rightarrow {}^3H_4$
	596		10	${}^1D_2 \rightarrow {}^3H_4$
	621		10	${}^1D_2 \rightarrow {}^3H_4$
$\text{Sm}^{3+}$	565	337	550	${}^4G_{5/2} \rightarrow {}^6H_{5/2}$
	601,612		550	${}^4G_{5/2} \rightarrow {}^6H_{7/2}$
	647		550	${}^4G_{5/2} \rightarrow {}^6H_{9/2}$
$\text{Eu}^{3+}$	596	337	1500	${}^5D_0 \rightarrow {}^7F_1$
	616		50	${}^5D_0 \rightarrow {}^7F_2$
	654		1500	${}^5D_0 \rightarrow {}^7F_3$
	702		1500	${}^5D_0 \rightarrow {}^7F_4$
	707		1500	${}^5D_0 \rightarrow {}^7F_4$
$\text{Gd}^{3+}$	312	266	2500	${}^6P \rightarrow {}^8S_{7/2}$
$\text{Tb}^{3+}$	383	266	325	${}^5D_3 \rightarrow {}^7F_6$
	415		325	${}^5D_3 \rightarrow {}^7F_5$
	437		325	${}^5D_3 \rightarrow {}^7F_4$
	489		2400	${}^5D_4 \rightarrow {}^7F_6$
	548		2400	${}^5D_4 \rightarrow {}^7F_5$
$\text{Dy}^{3+}$	478	337	120	${}^4F_{9/2} \rightarrow {}^6H_{15/2}$
	575		120	${}^4F_{9/2} \rightarrow {}^6H_{13/2}$
$\text{Ho}^{3+}$	549	337	1	${}^5S_2 \rightarrow {}^5I_8$
	665		1	${}^5F_3 \rightarrow {}^5I_7$
$\text{Er}^{3+}$	549	337	10	${}^4S_{3/2} \rightarrow {}^4I_{15/2}$
	559		10	${}^4S_{3/2} \rightarrow {}^4I_{15/2}$
$\text{Tm}^{3+}$	289	266	15	${}^1I_6 \rightarrow {}^3H_4$
	347		15	${}^1I_6 \rightarrow {}^3H_6$
	458		5	${}^1D_2 \rightarrow {}^3H_4$
	483		120	${}^1G_4 \rightarrow {}^3H_6$

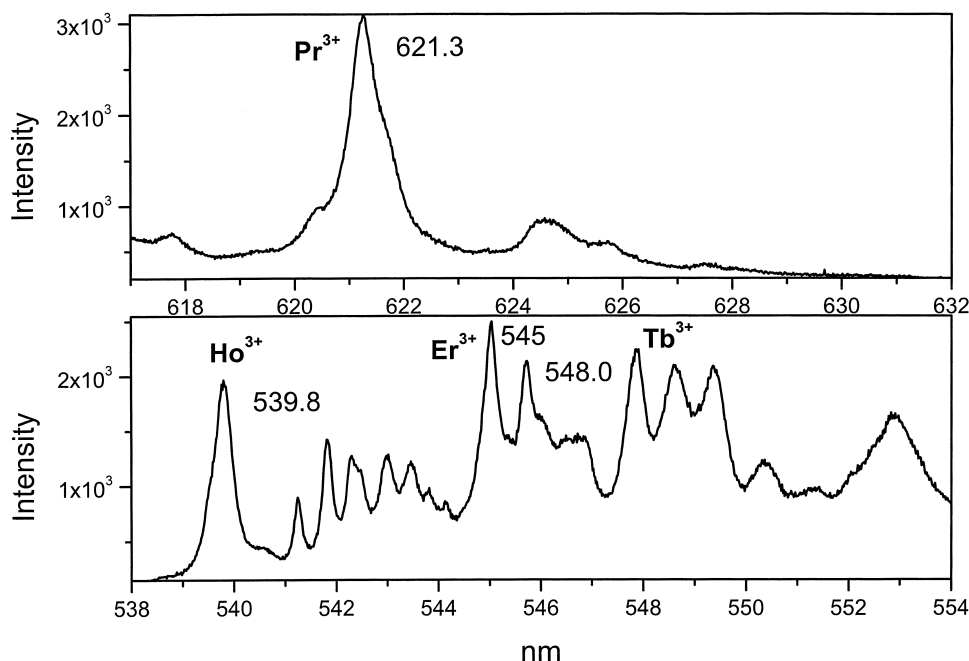


Fig. 6. Laser-induced luminescence spectra of natural zircon (Kola Peninsula, Russia) under 488 nm excitation.

individual ‘diagnostic’ lines, enabling confident identification of the spectrum possible. Luminescence lines of  $\text{Er}^{3+}$ ,  $\text{Ho}^{3+}$  and  $\text{Pr}^{3+}$  are clearly seen in high-resolution luminescence spectra of natural zircon (Fig. 6).

Electron transitions responsible for REE luminescence detected in natural zircon are presented in Table 2.

#### 4. Conclusions

We conclude that the combination of time-resolved spectroscopy under UV laser excitation and high-resolution spectroscopy with visible laser excitation enables to detect luminescence of  $\text{Ce}^{3+}$ ,  $\text{Pr}^{3+}$ ,  $\text{Sm}^{3+}$ ,  $\text{Eu}^{3+}$ ,  $\text{Tb}^{3+}$ ,  $\text{Gd}^{3+}$ ,  $\text{Dy}^{3+}$ ,  $\text{Ho}^{3+}$ ,  $\text{Er}^{3+}$  and  $\text{Tm}^{3+}$  in natural zircons.

#### Acknowledgements

The Open University of Israel Research Fund supported this work.

#### References

- [1] I. Babsail, N. Hamelin, P. Townsend, Nucl. Instrum. Methods Phys. Res. 859 (60) (1991) 1219–1225.
- [2] A. Taraschan, Luminescence of Minerals, Naukova Dumka, Kiev, 1978, in Russian.
- [3] I. Shinno, Mineral. J. 13 (1987) 239–253.
- [4] I. Shinno, J. Jpn. Assoc. Miner. Pet. Econ. Geol. 81 (1986) 433–445.
- [5] M. Gaft, J. Thermal Anal. 38 (1992) 2281–2290.
- [6] R. Reisfeld, Struct. Bond. 13 (1973) 53–152.
- [7] R. Reisfeld, C. Jorgensen, Lasers and Excited States of Rare-earths, Springer, Berlin, 1978.